Supporting Information

Brindley et al. 10.1073/pnas.1210925109

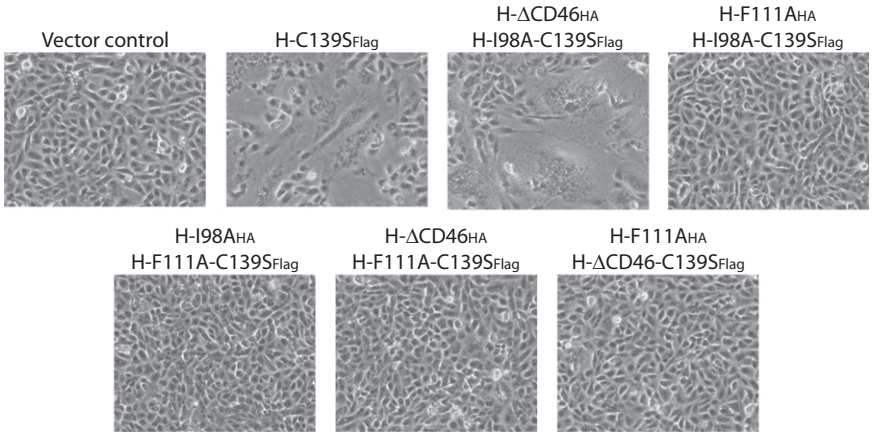

Fig. S1. Cysteine engineering to assess selective H transcomplementation on a homodimer/heterotetramer level. Microphotographs of Vero cells co-transfected with measles virus (MeV) fusion protein (F) and the specified attachment protein (H) constructs were taken 15 h posttransfection. (Magnification: 200×.)

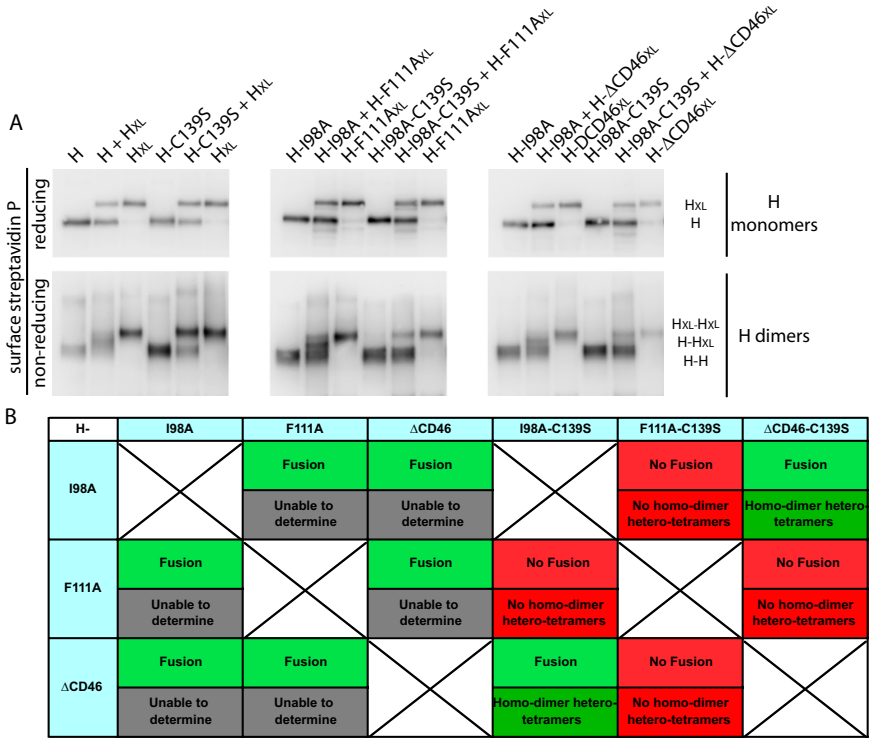

H-	I98A	F111A	ΔCD46	I98A-C139S	F111A-C139S	ΔCD46-C139S
I98A		Fusion Unable to determine	Fusion Unable to determine		No Fusion No homo-dimer hetero-tetramers	Fusion Homo-dimer hetero-tetramers
F111A	Fusion Unable to determine		Fusion Unable to determine	No Fusion No homo-dimer hetero-tetramers		No Fusion No homo-dimer hetero-tetramers
ΔCD46	Fusion Unable to determine	Fusion Unable to determine		Fusion Homo-dimer hetero-tetramers	No Fusion No homo-dimer hetero-tetramers	

Fig. S2. H-F111A homodimers are structurally distinct from homodimers of H or other H complementation groups. (*A*) Gel-fractionation of surface-exposed H under reducing and nonreducing conditions. Where indicated, H proteins contained a C-terminal single-chain antibody size tag (H_{XL}). The migration positions of H monomers (H, H_{XL}) and covalently linked dimers (H-H, H_{XL}-H_{XL}, H-H_{XL}) are highlighted. (*B*) Phenotype matrix of all H variants subjected to trans-complementation experiments. For each combination, fusion activity determined in cell-to-cell fusion assays and the ability to form homodimer hetero-tetramers are shown.

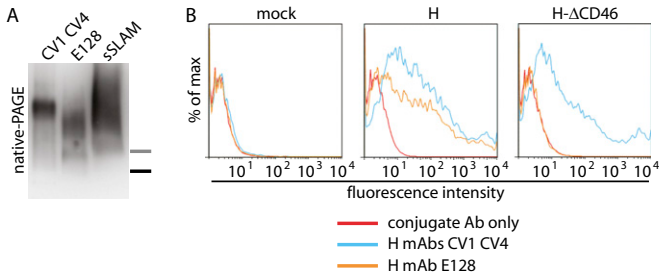

Fig. S3. Characterization of soluble proteinaceous H ligands. (*A*) Native-PAGE analysis of mAbs CV1 and CV4 and E128 and of soluble purified signaling lymphocyte activation molecule (sSLAM) demonstrates a similar mobility pattern in the absence of MeV H complexes. Immunoblots were decorated with α-mouse conjugate antiserum. For orientation, the mobility markers of the different-conformation MeV H tetramers (as in Fig. 3*C*) are shown. (*B*) Flow cytometric analysis of cells expressing MeV H or the H-ΔCD46 variant that lacks the ability to recognize the CD46 receptor. The mAb E128 epitope overlaps with the CD46 RBS, whereas mAbs CV1 and CV4 recognize distinct epitopes in the H head domain.

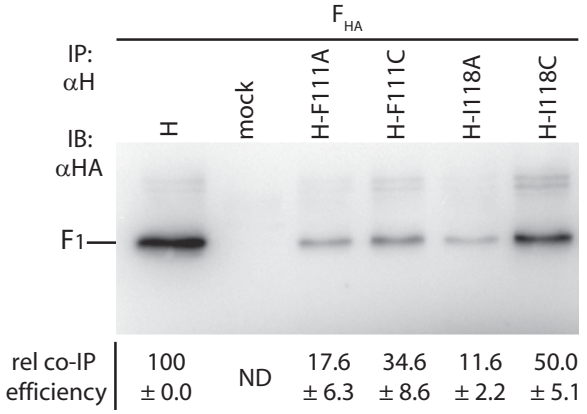

Fig. S4. Coimmunoprecipitation (co-IP) of surface-exposed MeV F_{HA} with MeV H. Surface-exposed glycoprotein complexes were chemically cross-linked with membrane-impermeable 3,3′-Dithiobis[sulfosuccinimidylpropionate] (DTSSP), followed by immunoprecipitation of H with an mAb mixture directed against the H ectodomain, SDS/PAGE, and immunoblotting with specific antibodies directed against the HA epitope. Cells expressing F alone served as specificity control (mock). Values below the immunoblots represent relative F coimmunoprecipitation efficiencies; averages of four independent experiments ± SEM are shown.

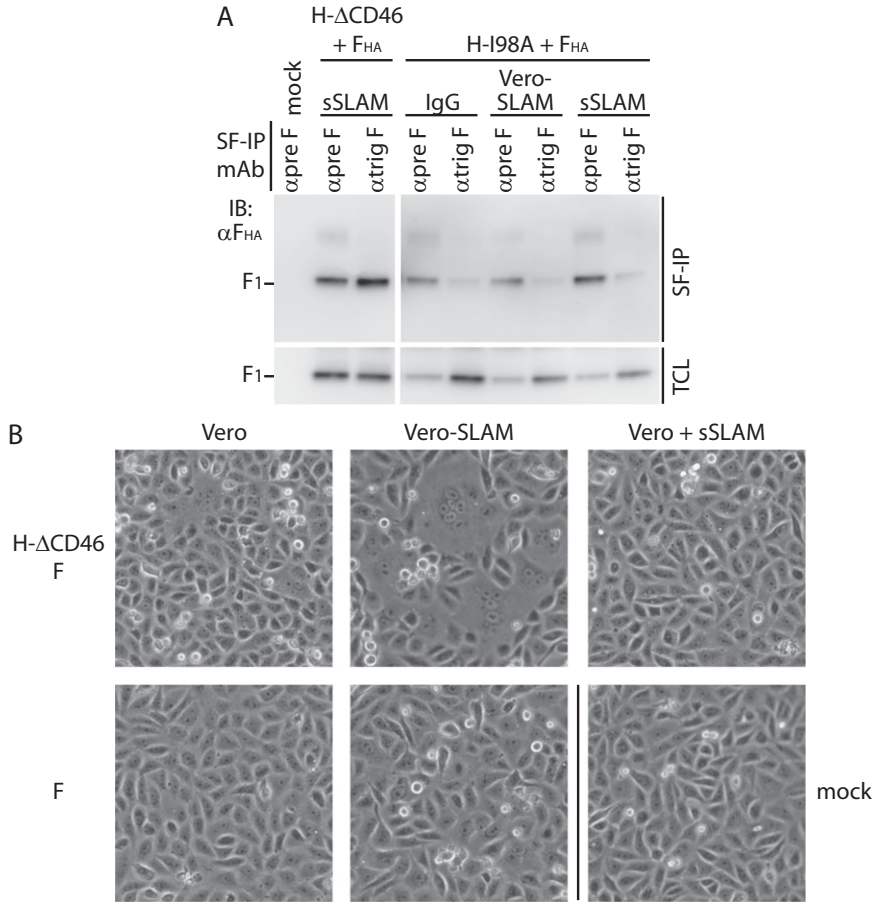

Fig. S5. Effect of soluble SLAM receptor on H-I98A F fusion complexes and syncytia formation. (*A*) Exposure of F-triggering–defective H-I98A tetramers to sSLAM does not lead to F reactivity with the α-trig F mAb, underscoring the specificity of the biochemical F-triggering assay. Surface immunoprecipitation of MeV F protein with conformation-dependent α-pre F and α-trig F mAbs after transfection of cells with plasmids encoding F and H-I98A. Transfected cells were overlaid with Vero-SLAM cells or exposed to sSLAM receptor as outlined in Fig. 8*B*. (*B*) Cells cotransfected with plasmids encoding MeV H-ΔCD46, F, and the N-terminal ($DSP_{1–7}$) GFP/renilla luciferase fragment were mixed with cells expressing the corresponding C-terminal ($DSP_{8–11}$) fragment and, where indicated, SLAM receptor. Specified cell populations were incubated continuously in the presence of sSLAM. Syncytium formation was assessed at a magnification of 200×. Representative fields of view are shown.

Table S1. Molecular characterization of mutant H protein variants

H construct*	H surface expression† (% of MeV H_{FLAG})	Receptor binding† (SLAM:H ratio; % of H_{FLAG})	Fusion activity‡ (% of MeV H_{FLAG})
H	106.2 ± 3.5	1.00 ± 0.04	108.6 ± 4.3
H_{FLAG}	100 ± 0.0	0.95 ± 0.08	100 ± 0.0
H_{HA}§	95.7 ± 16.2	1.00 ± 0.19	104.9 ± 5.3
H-C139S$_{FLAG}$	87.4 ± 5.6	0.86 ± 0.09	60.7 ± 8.5
H-I98A$_{HA}$§	113.1 ± 9.1	0.90 ± 0.03	4.3 ± 0.7
H-F111A$_{FLAG}$§	70.2 ± 2.6	1.06 ± 0.04	0.2 ± 0.1
H-F111A$_{HA}$§	85.3 ± 3.2	1.00 ± 0.10	0.2 ± 0.1
H-ΔCD46$_{FLAG}$§	109.1 ± 3.3	1.00 ± 0.03	9.1 ± 0.9
H-ΔCD46$_{HA}$	123.3 ± 2.5	0.90 ± 0.01	11.1 ± 1.3
H-I98A-C139S$_{FLAG}$	113.5 ± 8.1	0.96 ± 0.04	1.7 ± 1.5
H-F111A-C139S$_{FLAG}$	106.6 ± 8.4	0.92 ± 0.06	0.7 ± 0.5
H-ΔCD46-C139S$_{FLAG}$	57.5 ± 1.2	0.90 ± 0.07	0.1 ± 0.01
$H_{XL\text{-}FLAG}$	84.8 ± 6.2	ND¶	90.9 ± 5.2
$H_{XXL\text{-}FLAG}$	58.4 ± 6.8	0.44 ± 0.05	56.1 ± 3.9
H-F111A$_{XXL\text{-}FLAG}$	77.3 ± 12.8	0.54 ± 0.08	0.1 ± 0.01
H- ΔCD46$_{XXL\text{-}FLAG}$	36.9 ± 5.8	0.52 ± 0.05	3.5 ± 0.09
H-C139S$_{XXL\text{-}FLAG}$	69.2 ± 7.7	0.49 ± 0.15	30.3 ± 4.1
H-H71C$_{FLAG}$	103.6 ± 10.6	0.78 ± 0.12	18.2 ± 7.01
H-K72C$_{FLAG}$	61.3 ± 8.9	0.81 ± 0.09	0.3 ± 0.08
H-S73C$_{FLAG}$	150.3 ± 12.4	0.92 ± 0.05	118.7 ± 24.8
H-L74C$_{FLAG}$	122.2 ± 9.5	0.97 ± 0.08	100.7 ± 10.5
H-R110C$_{FLAG}$	96.6 ± 2.7	0.71 ± 0.17	0.4 ± 0.2
H-F111C$_{FLAG}$	139.3 ± 13.7	0.89 ± 0.04	0.5 ± 0.1
H-T112C$_{FLAG}$	149.6 ± 12.0	0.82 ± 0.15	10.7 ± 2.6
H-L114C$_{FLAG}$	150 ± 16.2	0.87 ± 0.09	0.1 ± 0.04
H-I118C$_{FLAG}$	148.6 ± 14.5	0.89 ± 0.07	108.0 ± 14.9
H-I122C$_{FLAG}$	9.0 ± 1.2	0.31 ± 0.10	0.4 ± 0.1
H-Y131C$_{FLAG}$	107.0 ± 15.0	0.77 ± 0.10	58.2 ± 10.7
H-D132C$_{FLAG}$	128.8 ± 4.6	0.82 ± 0.12	129.2 ± 13.1
H-N141C$_{FLAG}$	87.6 ± 7.2	1.05 ± 0.10	5.4 ± 0.5
H-P142C$_{FLAG}$	81.7 ± 13.0	0.94 ± 0.06	6.1 ± 1.7
H-P143C$_{FLAG}$	85.9 ± 13.9	0.92 ± 0.03	0.1 ± 0.04
H-E144C$_{FLAG}$	85.8 ± 11.2	0.87 ± 0.03	18.2 ± 3.2
H-R145C$_{FLAG}$	79.6 ± 11.3	0.86 ± 0.10	28.0 ± 3.9
H-I146C$_{FLAG}$	57.7 ± 14.6	0.74 ± 0.08	1.6 ± 0.4
H-K147C$_{FLAG}$	74.1 ± 7.3	0.84 ± 0.04	0.2 ± 0.06
H-L148C$_{FLAG}$	83.4 ± 8.3	1.04 ± 0.18	50.3 ± 9.9
H-D149C$_{FLAG}$	97.9 ± 4.6	0.91 ± 0.09	0.1 ± 0.07
H-Y150C$_{FLAG}$	96.9 ± 4.5	0.98 ± 0.02	4.9 ± 1.2
H-D151C$_{FLAG}$	97.1 ± 5.9	0.95 ± 0.13	62.1 ± 9.9
H-Q152C$_{FLAG}$	74.5 ± 5.4	1.00 ± 0.12	22.9 ± 8.6

ND, not determined.

*All constructs are based on H-Edm (1).

†Determined by flow-cytometric analysis of H expressing cells using H-specific antiserum; values are based on median fluorescence intensities, averages of at least three experiments ± SEM.

†Determined by flow-cytometric analysis of H expressing cells using soluble SLAM and H-specific antisera; values represent median fluorescence intensities, averages of at least three experiments ± SEM.

‡Determined by quantitative fusion assay in Vero cells, averages of at least three experiments ± SEM.

§Surface expression and receptor binding values as reported in ref. 2.

¶SLAM-binding activity of this H variant demonstrated in ref. 3.

1. Cathomen T, Naim HY, Cattaneo R (1998) Measles viruses with altered envelope protein cytoplasmic tails gain cell fusion competence. *J Virol* 72:1224–1234.
2. Brindley MA, Plemper RK (2010) Blue native PAGE and biomolecular complementation reveal a tetrameric or higher-order oligomer organization of the physiological measles virus attachment protein H. *J Virol* 84:12174–12184.
3. Hammond AL, et al. (2001) Single-chain antibody displayed on a recombinant measles virus confers entry through the tumor-associated carcinoembryonic antigen. *J Virol* 75: 2087–2096.